

Flash Carbonization of Biomass

Michael Jerry Antal, Jr.,* Kazuhiro Mochidzuki, and Lloyd S. Paredes

Hawaii Natural Energy Institute, School of Ocean and Earth Science and Technology,
University of Hawaii at Manoa, Honolulu, Hawaii 96822

We describe the ignition and control of a flash fire at elevated pressure (≈ 1 MPa) within a packed bed of biomass. The fire moves upward through the bed, against the downward flow of air, triggering the transformation of biomass into gas at elevated pressure, and charcoal with fixed-carbon yields that reach the thermochemical equilibrium “limit” in <30 min of reaction time. In a typical experiment 65% of the moist feedstock mass is converted into a combustible gas at 1 MPa, and 40% of the dry mass remains as charcoal, retaining as much as 66% of the energy content of the feedstock. Biomass feedstocks included woods (*Leucaena* and oak) and agricultural byproducts (macadamia nut shells and corncob). In the case of corncob, the fixed-carbon yield attained the theoretical limit (28%), and the bed was fully carbonized after 20 min. Some of these findings were unexpected. For example, thermochemical equilibrium calculations predicted a negligible influence of pressure on charcoal yields, but we observed considerable improvements at modest elevated pressures (e.g., 1 MPa). Furthermore, the fixed-carbon yields for oak wood and corncob in this work exceeded the yields obtained at similar elevated pressures *in the absence of air* within an electrically heated autoclave. Some qualitative kinetic explanations are offered to explain these unexpected results.

Introduction

Biocarbons (e.g., charcoal and carbonized charcoal) have been manufactured by man for more than 38 000 years^{1,2} and are among the most important renewable fuels in use today. Nevertheless, commercial technologies that carbonize biomass are remarkably slow and inefficient. A typical yield of charcoal manufactured from hardwoods in a Missouri kiln operated on a 7–12 day cycle is about 25 wt %.³ This charcoal has a fixed-carbon content of about 80 wt %; therefore, the process offers a fixed-carbon yield of about 20 wt %.⁴ Less efficient carbonization processes are widely employed in the developing world^{5–8} and are a contributor to the deforestation of many tropical countries. Also, because of pollution associated with inefficient carbonization processes, the charcoal fuel cycle is among the most greenhouse-gas-intensive energy sources employed by mankind.⁵

From a theoretical perspective, biomass carbonization should be efficient and quick. Thermochemical equilibrium calculations^{9–11} indicate that carbon is a preferred product of biomass pyrolysis at moderate temperatures, with byproducts of carbon dioxide, water, methane, and traces of carbon monoxide. To illustrate this result, we display in Figure 1a the products of cellulose pyrolysis in thermochemical equilibrium as a function of pressure at 400 °C. Cellulose is the dominant component of most biomass, and serves as a representative model compound in this discussion. The major trends displayed in Figure 1 are unchanged when the exact C, H, and O compositions of particular biomass species are employed in the thermochemical equilibrium calculations. At 1 MPa the yield of carbon from cellulose is 27.7 wt % (i.e., 62.4 mol % of cellulose carbon is converted into biocarbon) and is not significantly affected by pressure. Figure 1b displays the effects of temperature on the thermochemical equilibrium product yields at 1.0 MPa. Temperatures below 400 °C are primarily of theoretical interest since the rates of biomass carbonization are

very slow in this regime. At higher temperatures the yields of carbon, water, and methane decrease with increasing temperature, while those of carbon dioxide and carbon monoxide increase. In light of these results, we assume that the carbon yield realized under equilibrium conditions in the absence of oxygen at 400 °C and 1 MPa is the maximum (or near maximum) value that can be obtained when thermochemical equilibrium is established.

An energy balance on the thermodynamic process that creates the equilibrium product mixture at 400 °C and 1 MPa, and thereafter makes the products available at room conditions, offers the following insights (see Figure 2). Assuming constant specific heat (1.38 kJ/kg·K), 518 kJ/kg of cellulose (kJ/kg-cell) or 3% of the higher heating value (HHV) of the cellulose (17.4 MJ/kg-cell) must be supplied from an external heat source to elevate the substrate temperature to 400 °C, but no work is required to augment its pressure since the solid is idealized as incompressible. This energy input to the process is illustrated as the top bar in Figure 2. The attainment of equilibrium releases 6.7% (1167 kJ/kg-cell) of the HHV of cellulose as the exothermic heat of reaction, and the evolution of gaseous products (idealized as ideal) at 1 MPa does 176 kJ/kg-cell of work on the environment. Further work (257 kJ/kg-cell) is recovered by an isentropic expansion of the gas (with idealized constant specific heats) to 0.1 MPa and 149 °C, and heat is recovered from the gas (852 kJ/kg-cell or 4.9% of the HHV of the cellulose) and carbon (74 kJ/kg-cell or 0.4% of the HHV of the cellulose) by cooling to 25 °C. The carbon product retains 52.2% (9078 kJ/kg-cell) of the HHV of the cellulose, and 36.3% (6313 kJ/kg-cell) is captured by the gas products (primarily methane). These energy outputs of the process are illustrated as the bottom bar in Figure 2. We remark that the highest measured value for the exothermic heat of pyrolysis of cellulose—in a closed crucible that developed considerable pressure within a differential scan-

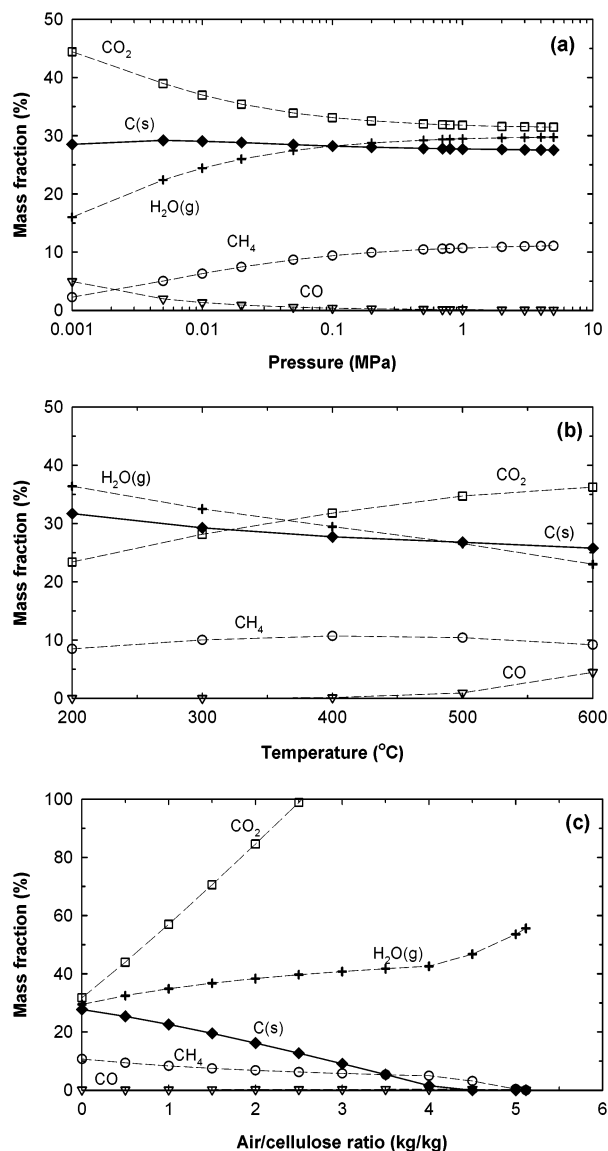


Figure 1. (a) Effects of pressure on the products of cellulose pyrolysis following the attainment of thermochemical equilibrium at 400 °C. (b) Effects of temperature on the products of cellulose pyrolysis following the attainment of thermochemical equilibrium at 1 MPa. (c) Effects of air–biomass ratio on the products of cellulose combustion following the attainment of thermochemical equilibrium at 1 MPa, 400 °C. (◆) C(s), (□) CO₂, (▽) CO, (○) CH₄, and (+) H₂O(g).

ning calorimeter (DSC)—was 660 kJ/kg-cell (i.e., 3.8% of the HHV of cellulose).¹² In light of the fact that the exothermic pyrolysis reaction proceeds with a large increase in entropy (due to the formation of gas), it is clear that equilibrium strongly favors the formation of product carbon and byproduct gases. We remark that chemical reactions, which involve large releases of both heat and entropy, usually proceed quickly following initiation.

Webster¹³ defines the adjective “flash” as follows: “of sudden origin and short duration <a ~ fire>”. In this paper we show how to ignite and control a flash fire at 1 MPa within a packed bed of biomass. Heat released by the fire triggers the transformation of biomass into carbon with yields that can reach the thermochemical equilibrium “limit” in <30 min of reaction time. On a carbon basis, about 60% of the carbon in the feedstock is converted into charcoal fixed carbon. On the other hand, about two-thirds of the feedstock’s moist mass is

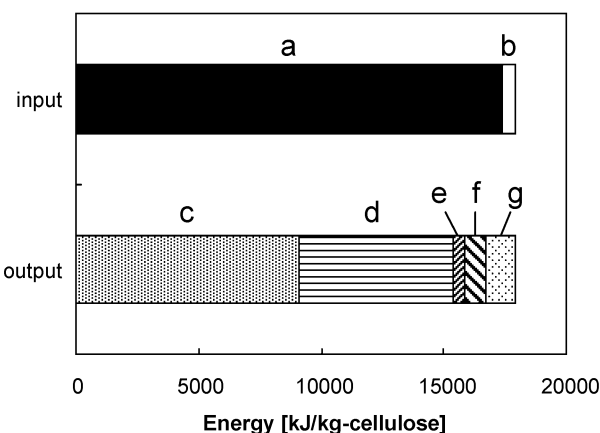


Figure 2. Energy balance for the pyrolysis of cellulose at 400 °C and 1 MPa: a, cellulose HHV; b, sensible heat requirement; c, carbon combustion energy content; d, gas combustion energy content; e, available work via gas expansion; f, sensible heat available in carbon and gas products; g, carbonization exotherm.

converted into a combustible gas at elevated pressure. This gas can be expanded through a turbine to generate shaft power. If necessary, two or more flash carbonization reactors can be operated sequentially to provide a steady flow of gas to the turbine. Consequently, the flash carbonization process functions as both a gasification process and a carbonization process. From the standpoint of thermochemical equilibrium, the high yields of charcoal and fixed carbon reported in this paper are a surprise. As illustrated in Figure 1c, the presence of oxygen (air) in the reaction mixture reduces the thermochemical equilibrium yield of carbon relative to the values displayed in Figure 1a,b. The steep decline in the solid carbon yield with increasing air–cellulose ratio indicates that while reaching equilibrium, oxygen preferentially attacks carbon instead of methane. Kinetic phenomena that result from the unique pyrolytic properties of biomass are the root cause of the unexpectedly high yields. In what follows we offer a qualitative discussion of these phenomena and their impacts upon flash carbonization. We also provide an assessment of the carbon distribution between the various products of flash carbonization of *Leucaena* wood.

Apparatus and Experimental Procedures

Biomass feedstocks employed in this study are listed in Table 1. Waste oak (*Quercus spec.*) wood floorboards, used for the commercial production of charcoal, were supplied by the Cowboy Charcoal Co. Air-dried, debarked *Leucaena leucocephala* logs and corncob grown on Oahu were provided by Prof. J. Brewbaker (U. Hawaii). Data listed in Table 1 are for *Leucaena* log #9. In one experiment (LW-A2) we used *Leucaena* log #3, whose ash content was only 1.65%. Both the oak and the *Leucaena* wood pieces were cut to a uniform size of about 10 × 2.5 × 2.5 cm to facilitate loading. We remark that moist wood logs were successfully carbonized in a pressurized, high-yield charcoal pilot reactor that was operated on campus until about 4 years ago.^{4,14} Macadamia nut shells (“macshells”) were collected on the Big Island of Hawaii. Table 1 also displays the “ultimate” (elemental) analyses of each feed. These analyses of representative subsamples of the actual feeds employed in this work were made by the Huffman Laboratories, Inc. We remark that these elemental analyses differ significantly from analyses of feeds (i.e., *Leucaena*,

Table 1. Feedstock Analyses: Leucaena Wood (LW), Oak Wood (OW), Corncob (CC), and Macadamia Nut Shell (MS)

ID	MC ^a (%)	ash ^b (%)	ultimate analysis ^c (%)					ash	HHV ^c (MJ/kg)	SABR ^d (kg/kg)
			C	H	O	N	S			
LW	13.1	2.34	48.47	5.90	42.41	0.51	0.08	3.49	18.1	5.76
OW	8.67	0.27	46.44	6.45	47.42	0.10	0.02	0.39	17.7	5.50
CC	13.9	1.17	43.42	6.32	46.69	0.67	0.07	2.30	17.4	5.14
MS	9.37	0.41	52.28	5.65	42.33	0.29	0.06	0.58	20.7	6.12

^a Dry basis moisture content using ASTM E 1756-95. ^b ASTM E 1755-95. ^c Dry basis values measured by Huffman Laboratories, Inc., USA. ^d Stoichiometric air/biomass ratio.

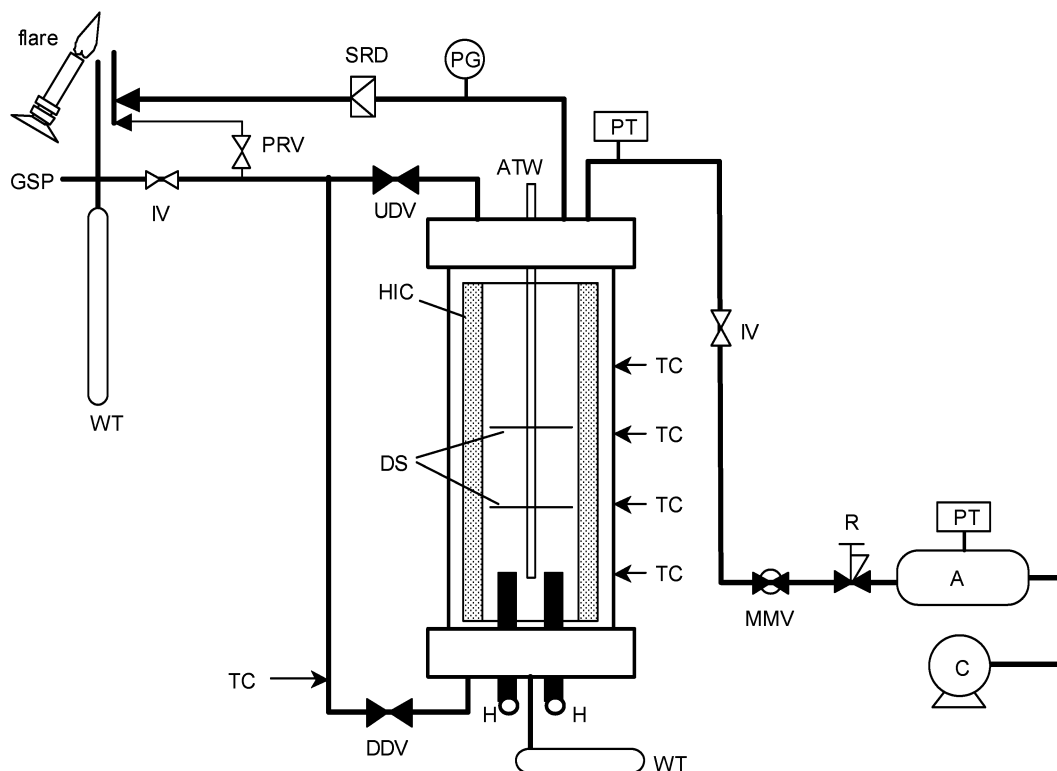


Figure 3. Schematic diagram of the flash carbonization reactor. A, air accumulator; ATW, annular thermocouple well with 5 thermocouples; C, compressor; DDV, downdraft valve; DS, disk separator; GSP, gas sampling port; H, electric heater; HIC, heat-insulating canister; IV, isolation valve; MMV, micrometer valve; PG, pressure gauge; PRV, pressure relief valve; PT, pressure transducer; R, regulator; SRD, safety rupture disk; TC, thermocouple; UDV, updraft valve; WT, water trap.

oak, corncobs, and macshells) employed in our earlier work.⁴ We presume that these differences represent the inherent variability of biomass feedstocks from one year, location, etc. to the next. In what follows we neglect the feedstock nitrogen and sulfur content (see Table 1) in comparing thermochemical equilibrium yields with experimental results. This approximation has no significant effect on the carbon yields that are the focus of this paper. In some cases we represent results on an ash-free basis (e.g., the fixed-carbon yield), whereas in others we employ a whole dry biomass basis (e.g., the calculated stoichiometric air–biomass ratio). The listed units of the results indicate the basis employed.

In a typical experiment a measured amount (0.5–1.4 kg) of feedstock is placed inside a cylindrical canister, divided into three sections by metal screens, with 5 type K thermocouples positioned along the canister's centerline. Then the canister is loaded into a vertical pressure vessel (autoclave) that is subsequently pressurized to 1.1 MPa (150 psig) by air (see Figure 3). Electric power (0.2 kW·h) is delivered to two heaters at the bottom of the autoclave. Ignition occurs after a few minutes and the heaters are turned off. The total power consumption (ca. 0.4 kW·h/kg of charcoal) is almost a factor of 10 less than that employed in our earlier work¹⁵ and will be

reduced further when larger autoclaves enable the same power input to ignite a flash fire within a much larger bed of biomass. Gas is released from the bottom of the autoclave to maintain the pressure at its initial value while the temperature of the bottom of the bed rises to a maximum value. This starved-air ignition step creates a shallow bed of carbon at the bottom of the canister. Then about 28 g/min of air is delivered to the top of the reactor while combustion gas is vented from the bottom. The flame front moves up the bed, against the flow of air, triggering the conversion of biomass into carbon. When sufficient air has been delivered to ensure carbonization of the bed, the air flow is halted and the autoclave is depressurized and permitted to cool. Subsequently, each section is equilibrated in the open air and weighed and a representative carbon subsample taken from each section is subjected to proximate analysis according to ASTM D1762-84. Some selected charcoal samples are also subject to elemental analysis (Huffman Laboratories, Inc.).

In contrast with our earlier work,⁴ the exhaust gas cannot be ignited by a flame. No tar droplets were visible in the gas and no tar has accumulated in the hood vent system that services the autoclave. During each experiment, samples of the exhaust gas from the

Table 2. Results of Flash Carbonization: Air-Dried Leucaena Wood (LW-A), Oven-Dried Leucaena Wood (LW-O), Oak Wood (OW), Corncob (CC), and Macadamia Nut Shell (MS)

ID	section	proximate analysis (%)			y_{char} (%)	y_{fc} (%)	HHV _m ^b (MJ/kg)	HHV _e ^c (MJ/kg)	η_{char} (%)
		VM	fC	ash					
LW-A1	top	9.6	87.1	3.3	34.7	31.0		31.6	60.6
020214	middle	12.2	84.1	3.7	35.9	30.9		31.1	61.8
	bottom	36.7	61.0	2.3	45.3	28.3		28.8	72.2
	average ^a	24.7	72.5	2.9	40.0	29.7		30.0	66.3
LW-A2	top	4.4	94.1	1.5	29.0	27.8		34.1	54.7
020930	middle	6.4	92.1	1.5	30.1	28.2		33.7	56.1
	bottom	6.9	91.5	1.6	29.4	27.3		33.6	54.6
	average ^a	6.0	92.4	1.5	29.5	27.7	33.5	33.8	55.1
LW-O	top	5.8	90.3	3.8	32.9	30.4		31.8	57.7
020311	middle	12.6	83.7	3.6	36.6	31.4		31.1	63.0
	bottom	21.4	75.0	3.6	38.8	29.8		30.1	64.6
	average ^a	15.8	80.6	3.6	36.8	30.4		30.7	62.6
OW-1	top	9.8	89.4	0.8	33.4	29.9		33.3	62.8
020221	middle	11.6	87.8	0.7	27.4	24.2		33.1	51.2
	bottom	9.9	89.2	0.9	35.2	31.5		33.3	66.2
	average ^a	10.3	88.9	0.8	32.6	29.1		33.3	61.2
OW-2	top	15.3	83.9	0.8	34.1	28.6		31.8	61.2
020327	middle	18.1	81.4	0.5	34.2	27.9		31.6	61.0
	bottom	24.6	75.0	0.4	36.5	27.5		30.9	63.7
	average ^a	20.0	79.5	0.5	35.1	28.0	31.1	31.4	62.2
CC	top	17.5	80.1	2.4	33.4	27.0		31.0	59.3
020204	middle	13.7	83.7	2.6	32.3	27.4		31.4	58.1
	bottom	11.0	86.1	3.0	33.5	29.1		31.5	60.5
	average ^a	13.6	83.7	2.7	33.1	28.0	30.9	31.3	59.5
MS	top	2.7	96.4	0.9	31.0	30.0		34.6	51.8
020510	middle	5.7	93.4	0.9	36.6	34.3		34.1	60.2
	bottom	16.5	82.6	0.9	35.5	29.4		32.1	55.0
	average ^a	9.8	89.3	0.9	34.5	30.9	33.3	33.3	55.5

^a Weighted average. ^b Measured by Huffman Laboratories, Inc. ^c Estimated according to the correlation of Cordero et al.

reactor were collected. These samples were injected into gastight test tubes (vacutainers) for short-term storage. The gas composition (hydrogen, oxygen, nitrogen, carbon monoxide, carbon dioxide, and some hydrocarbons) was measured by a GC-TCD system (Hewlett-Packard 5890 Series II with Alltech Carbospher 80/100 column, operating at 35 °C for 4.0 min, followed by a 25 °C/min ramp to 350 °C and a 1.4 min hold at 350 °C). The carrier gas was a mixture of 8% hydrogen in helium. A standard gas mixture was used for calibration, and another standard gas mixture (method verification standard) was used to verify the accuracy of the calibration.

Results and Discussion

We define the charcoal yield $y_{\text{char}} = m_{\text{char}}/m_{\text{bio}}$, where m_{char} is the dry mass of product charcoal and m_{bio} is the dry mass of the feedstock. Unfortunately, this representation of the carbonization efficiency is intrinsically vague because the chemical composition of charcoal is not defined. A more meaningful measure of the carbonization efficiency is given by the fixed-carbon yield $y_{\text{fc}} = y_{\text{char}} \times \{\% \text{ fC}/(100 - \% \text{ feed ash})\}$, where % fC is the percentage of fixed-carbon content of the charcoal and % feed ash is the percentage of ash content of the feed.⁴ This yield represents the efficiency realized by the pyrolytic conversion of ash-free organic matter in the feedstock into a relatively pure, ash-free carbon. Finally, we define the energy conversion efficiency $\eta_{\text{char}} = y_{\text{char}} \times (\text{HHV}_{\text{char}}/\text{HHV}_{\text{bio}})$, where HHV_{char} is the HHV of the charcoal and HHV_{bio} is the HHV of the feedstock. Because the determination of the HHV can be expensive when many samples are tested, we sometimes employ the correlation¹⁶ proposed by Cordero et al.: $\text{HHV} (\text{MJ/kg}) = 0.3543\% \text{ fC} + 0.1708\% \text{ VM}$. This correlation offers a good fit ($R^2 = 0.938$) to measured HHV data for

a representative selection of biocarbons produced by flash carbonization.

The scientific literature concerning biomass carbonization spans 150 years^{17,18} and stands on a foundation developed over 38 millenia.¹ No record exists of a fixed-carbon yield from biomass that exceeds the thermochemical equilibrium value for the carbon yield. Evidently, the pyrolytic yield of carbon from biomass approaches the equilibrium value from below; consequently, we refer to this value as the thermochemical equilibrium "limit" for the carbon yield. As discussed earlier, we calculate the "limit" value at 400 °C and 1 MPa in the absence of oxygen. These reaction conditions offer near-optimum yields of carbon from biomass when equilibrium is established.

Table 2 summarizes the results of the flash carbonization of biomass materials listed in Table 1. Oak and Leucaena (a nitrogen fixing tree) are popular feedstocks for the production of charcoal. In experiment OW-1 the oak was ignited at 3.0 MPa and pressure was gradually reduced thereafter to 1.1 MPa with a cessation of airflow after 21 min. The bottom temperatures (near the heaters) quickly rose (see Figure 4a) to values near 500 °C. The flame front moved up the bed, causing the middle, mid-top, and top temperatures to successively increase, reaching values near 600 °C. On the basis of the C, H, and O composition of the oak (Table 1), the thermochemical equilibrium limit for the fixed-carbon yield is 29.6 wt %.⁴ The experimental mass-weighted average fixed-carbon yield of this experiment (see Table 2) was 98% of the theoretical limit (see Figure 5), representing the transformation of 62% of the feedstock's carbon into fixed carbon. Corroborating this result, the energy content of the charcoal product was 61.2% of the dry oak feed. Note the uniformity of the charcoal with a range of volatile matter contents from

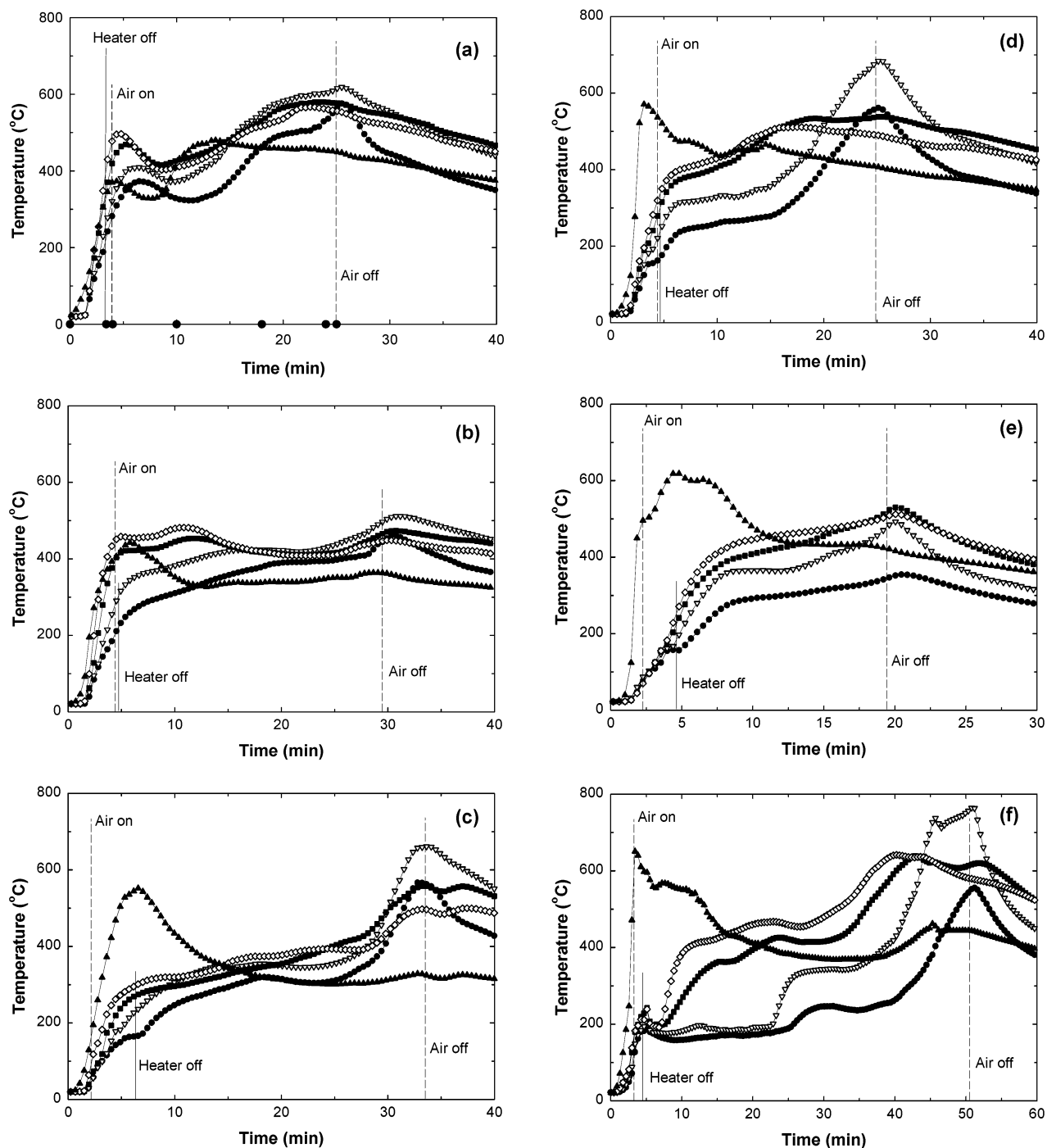


Figure 4. Measured centerline temperature profiles during the (a) oak wood 1, (b) oak wood 2, (c) air-dry *Leucaena* wood, (d) oven-dry *Leucaena* wood, (e) corncob, and (f) macadamia nut shell flash carbonization runs. (●) Top, (▽) mid-top, (■) middle, (◇) mid-bottom, and (▲) bottom.

9.8 to 11.6%. These results represented an unexpected, significant improvement over our earlier work that employed an electrically heated retort and achieved only 88% of the limit value for the fixed-carbon yield from oak after 300 min of reaction time from a cold start.⁴ In experiment OW-2 the oak ignited at 1.5 MPa after 5 min of heating, and pressure was gradually reduced to 1.1 MPa while combustion gas was released from the bottom of the autoclave. The bottom temperature quickly rose (see Figure 4b) to 450 °C and then fell to about 350 °C. As the flame front moved up the bed, the temperatures successively increased to values near 500 °C. Airflow was halted after 25 min. The measured

average value of the fixed-carbon yield was 95% of the thermochemical equilibrium limit, and the charcoal product retained 62.2% of the energy of the dry wood feed. Again, we call attention to the uniformity of the charcoal with volatile matter contents ranging from 15.3 to 24.6%.

In experiment LW-A1 the air-dry, debarked *Leucaena* wood was ignited at 1.1 MPa and pressure was held at that value throughout the run. Figure 4c displays the temperature profiles observed during the run. All temperatures exceeded 500 °C, and the mid-top temperature reached 640 °C. In this experiment (and some others) the top-temperature peak was lower than the mid-top

Table 3. Summary of the Air Input and the Theoretical y_{FC} for Each Run

	feedstock, dry-basis (kg)	P_{initial}^a (MPa)	P_{reaction}^b (MPa)	delivered air ^c		total air ^d		$y_{\text{FC}}(t)^f$ (%)
				ABR ^e (kg/kg)	λ	ABR ^e (kg/kg)	λ	
LW-A1	1.231	1.18	1.06	0.76	0.132	0.98	0.170	29.44
LW-A2	0.898	1.12	1.02	1.23	0.213	1.52	0.263	26.02
LW-O	1.170	1.50	1.01	0.53	0.092	0.82	0.143	30.37
OW-1	1.183	2.92	1.05	0.53	0.096	1.06	0.193	24.52
OW-2	1.247	1.66	1.03	0.59	0.106	0.91	0.165	25.34
CC	0.437	1.17	1.08	1.16	0.225	1.77	0.345	17.78
MS	1.100	1.16	1.06	1.28	0.159	1.53	0.189	29.20

^a Initial pressure for ignition. ^b Mean pressure during carbonizing reaction. ^c Delivered after ignition. ^d Initial amount in reactor + delivered. ^e Air–biomass ratio. ^f Theoretical y_{FC} at each total ABR.

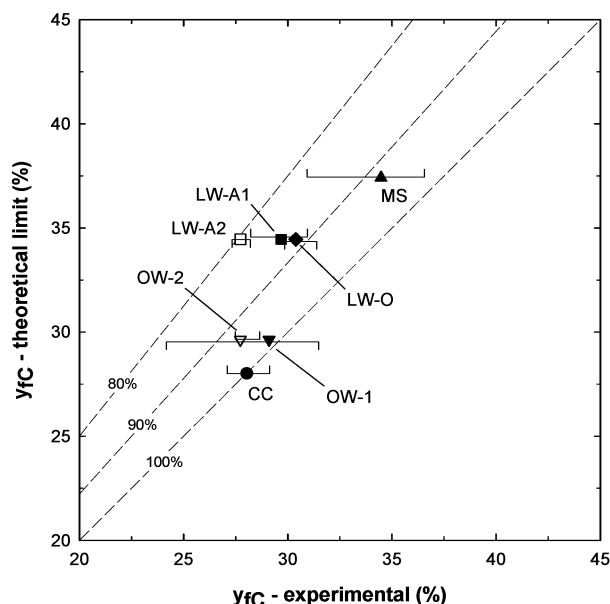


Figure 5. Parity plot displaying the experimental, mass-average value and the associated range of fixed-carbon yields vs the theoretical thermochemical equilibrium value ("limit") for all feedstocks. (■) Leucaena wood air-dried #1 (LW-A1), (◆) Leucaena wood oven-dried (LW-O), (▽) oak wood #1 (OW-1), (▼) oak wood #2 (OW-2), (●) corncob (CC), and (▲) macshell (MS).

temperature because bed shrinkage during carbonization caused the top of the bed to fall below the top thermocouple. High yields of charcoal (40.0%) and fixed carbon (29.7%) were realized in this run with $\eta_{\text{th}} = 66.3\%$. Over 59% of the feedstock's carbon was converted into fixed carbon, and 65% of the moist mass of Leucaena loaded into the reactor was gasified. Experiment LW-A2 was executed to produce metallurgical-grade charcoal. The reaction conditions were the same as those of LW-A1 except that sufficient air was fed to the reactor (see Table 3) to realize peak temperatures near 800 °C (not displayed). As expected, the VM content of this charcoal was very low with values between 4.4 and 6.9%. The relatively low fixed-carbon yield (80% of the theoretical value) realized in this experiment was the price paid to obtain a nearly pure carbon product.

Remarkably, the use of oven-dry, debarked Leucaena as feedstock (experiment LW-O) had little effect on the measured temperature profiles (Figure 4d), the fixed-carbon yield (30.4%), and the charcoal energy-conversion efficiency (62.6%). Apparently, the carbonization exotherm combined with the combustion of the pyrolysis gas released more than enough heat to dry the air-dry feed employed in experiment LW-A1. This unexpected result shows that a predrying step is not needed to realize high carbonization efficiencies from some moist

feedstocks. Furthermore, we remark that we have successfully flash-carbonized coarsely ground sawdust with a moisture content of 50% (wet basis). Nevertheless, it is evident that the reaction time of oven-dried Leucaena was significantly shorter than that of the air-dried wood.

Corn stover (including cobs) is the most plentiful agricultural residue in the United States. The cob is a particularly attractive feedstock for carbonization: at 1.2 MPa it ignited after 2 min of heating, and airflow to the autoclave was halted after 18 min. As displayed in Figure 4e, all temperatures in the bed (but not the top thermocouple, which was well above the bed in this run) reached 500 °C before the run was terminated. The fixed-carbon yield was 100% of the thermochemical equilibrium limit with $\eta_{\text{char}} = 59.5\%$. This remarkable result represents a substantial improvement over our earlier work with an electrically heated autoclave that realized <70% of the limit value for the fixed-carbon yield from cob after more than 300 min of reaction time.⁴ In this run 63% of the cob's carbon was converted to charcoal fixed carbon, and 71% of the cob's moist mass was gasified. The volatile matter contents of the three sections in this experiment increased somewhat from bottom to top, whereas they decreased in the other runs. It has been our experience that the material at the bottom of the canister—which rests upon the heavy bottom flange of the pressure vessel that remains cold during the entire run—often does not carbonize as fully as the material higher in the canister. This problem may be alleviated in a larger reactor with a smaller surface-to-volume ratio.

Macadamia nut shells are either burned in boilers or sent to landfill on the Big Island of Hawaii. In experiment MS, the shells were ignited at 1.1 MPa and the pressure was held at that level during the 47 min of airflow to the autoclave. The very rapid increase of the bottom temperature in this run (see Figure 4f) may have caused us to turn off the heaters prematurely, as evidenced by the low mid-top and top temperatures during the first 30 min of heating. But eventually the mid-top temperature approached 800 °C, giving rise to the very high fixed-carbon contents displayed in Table 2 and a fixed-carbon yield (30.9%) that exceeded 90% of the theoretical value (see Figure 5). In this run 59% of the macshell's carbon was converted to charcoal fixed carbon, and 55.5% of the macshell's calorific value was retained in the charcoal.

The high charcoal and fixed-carbon yields reported above—which were obtained by subjecting biomass to a flash fire at elevated pressure—were unexpected. Figure 6a (analogous to Figure 1c) displays the effect of increasing air on the product composition from Leucaena wood and air after the attainment of thermochemical equilibrium. Note how quickly the carbon yield

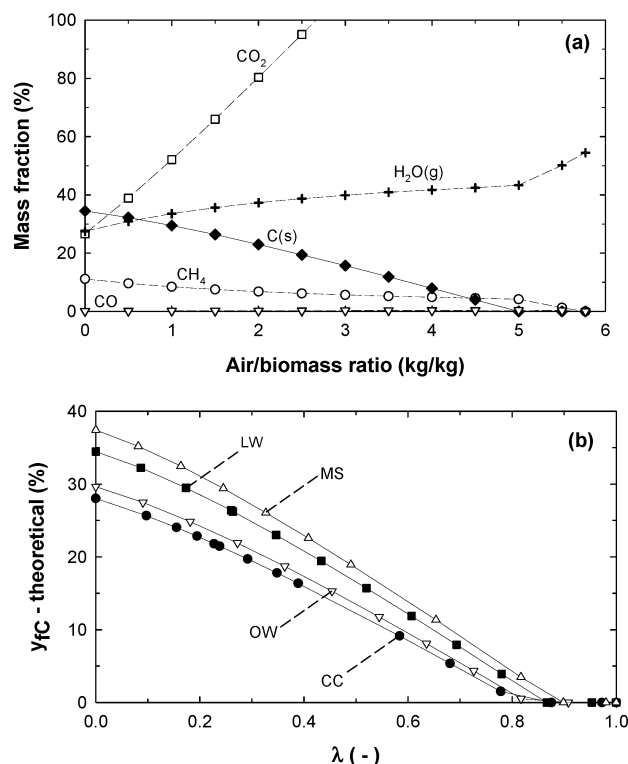
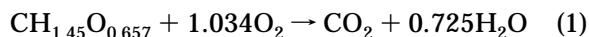


Figure 6. (a) Effects of air–biomass ratio on the products of Leucaena wood combustion following the attainment of thermochemical equilibrium at 400 °C and 1 MPa. (◆) C(s), (□) CO₂, (▽) CO, (○) CH₄, and (+) H₂O(g). (b) Effects of λ on the carbon yield from each feedstock following the attainment of thermochemical equilibrium at 400 °C and 1 MPa. (■) Leucaena wood, (▽) oak wood, (●) corncob, and (△) macshell.

decreases as the air–biomass ratio (i.e., air–fuel ratio) increases. We define $\lambda = (\text{actual air–biomass ratio})/(\text{stoichiometric air–biomass ratio})$, where the stoichiometric air–biomass ratio (SABR) is given in Table 1 for the biomass feedstocks employed in this work. For example, in the case of Leucaena wood the elemental analysis (Table 1) gives values C:H:O = 48.47:5.90:42.41 (wt %); therefore, the apparent composition formula of Leucaena can be written as CH_{1.45}O_{0.657} (unit MW = 23.98), and the stoichiometric equation for complete combustion of Leucaena is



From this equation the stoichiometric oxygen demand is 1.38 g of O₂/g of biomass (ash-free), or 1.34 g of O₂/g of biomass (i.e., 5.76 kg of air/kg of biomass), as given in Table 1. Figure 6b details the strong effect of increasing λ on the equilibrium carbon yield from each of the biomass feedstocks employed in this work. Although the flash carbonization experiments summarized in Table 2 involved values of $\lambda \geq 0.143$ (see Table 3), a comparison of the parity plot (Figure 5) for flash carbonization with that of our earlier work (involving an electrically heated retort with $\lambda \approx 0$) reveals improved fixed-carbon yields with the flash process for the oak, macshell, and corncob feedstocks and similar yields for Leucaena. For example, in Run LW-A2 the air/biomass ratio = 1.52 kg of air/kg of biomass and $\lambda = 1.52/5.76 = 0.263$, where we assume that the air available for combustion includes both the initial air present in the autoclave at elevated pressure and the

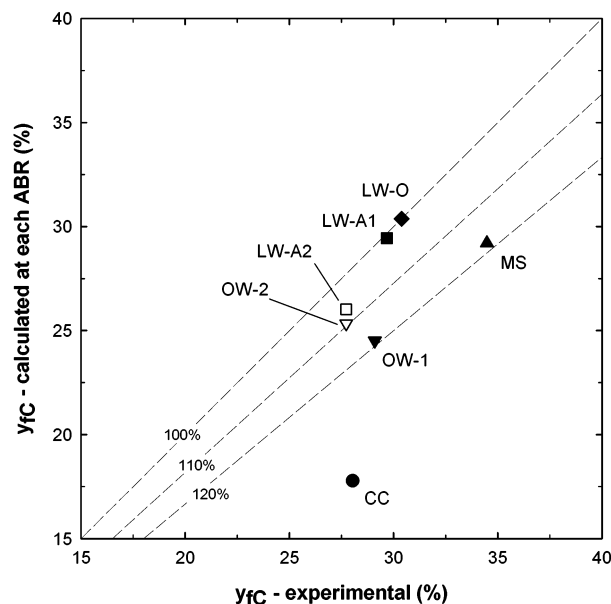
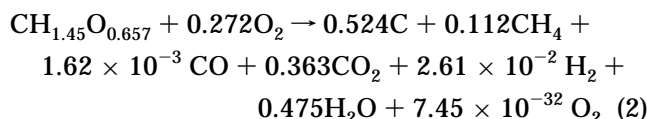
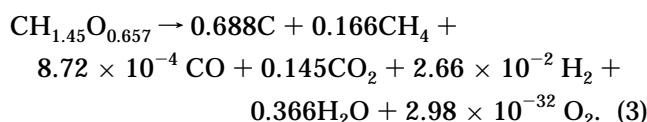


Figure 7. Parity plot displaying the experimental, mass-average value of fixed-carbon yields vs the value calculated at each ABR for all feedstocks. (■) Leucaena wood air-dried #1 (LW-A1), (□) Leucaena wood air-dried #2 (LW-A2), (◆) Leucaena wood oven-dried (LW-O), (▼) oak wood #1 (OW-1), (▽) oak wood #2 (OW-2), (●) corncob (CC), and (▲) macshell (MS).

air delivered to the autoclave during the experiment (see Table 3). Considering the amount of oxygen present at the air/biomass ratio of 1.52, a thermochemical equilibrium calculation gives the following result:



In eq 2 the value of y_{FC} is 26.2%. On the other hand, the measured experimental value of y_{FC} was 27.7% (see Table 2). Thus, the experimental value exceeds the predicted value by 6%. Now, if we employ a thermochemical equilibrium calculation with no oxygen at $T = 400$ °C and $P = 1$ MPa to predict the pyrolytic equilibrium composition and the limiting value of y_{FC} , we obtain



Thus, the limiting value of y_{FC} is 34.5% and this experiment realized a fixed-carbon yield that was 80% of the theoretical limit. In Figure 7 we display a parity plot that compares the predicted carbon yield for each flash-carbonization experiment (based on the assumption of thermochemical equilibrium including the air feed) with the experimentally measured value. The experimental yield exceeded the predicted yield in all cases (except LW-O), and for corncob the experimental yield was 57% larger than the predicted equilibrium value. These results clearly illustrate mass-transfer limitations that enable oxygen in air at elevated pressure to attack the gaseous pyrolysis products while sparing the solid carbon.

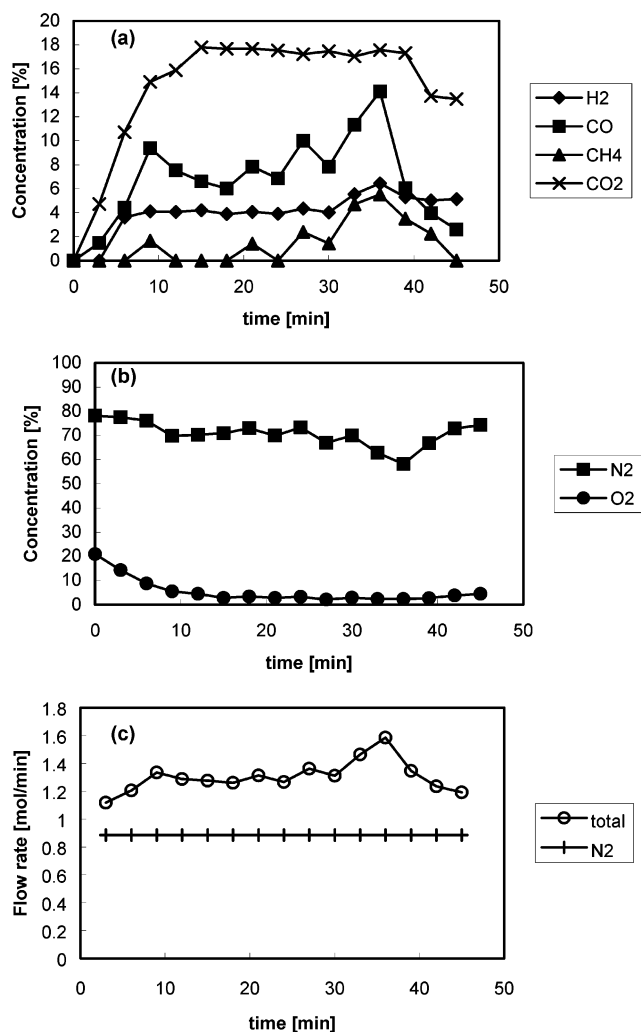


Figure 8. (a) GC analyses of the effluent pyrolysis gas products of Run LW-A2 and (b) GC analyses of the nitrogen and oxygen present in the effluent of Run LW-A2. (c) Measured flow rate of nitrogen entering the reactor and calculated total flow rate of the gases leaving the reactor.

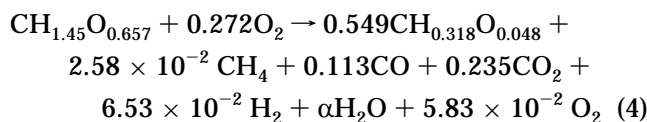
Although air was delivered to the reactor at a constant rate during these experiments, the pyrolytic evolution of gaseous products caused the flow of the exhaust gas to vary. To close the carbon balance for a representative experiment (Run LW-A2), we assumed the nitrogen present in air to be inert and used variations in the measured concentration of nitrogen in the exhaust gas to calculate the instantaneous flow rate of the exhaust gas. Figure 8a,b displays GC analyses of the effluent gaseous products and changes in the concentrations of nitrogen and oxygen during the run. Figure 8c displays the estimated flow rate of the effluent gas as calculated from the known flow rate of nitrogen into the reactor and the measured concentration of nitrogen in the effluent (Figure 8b). We used the estimated flow rate to make a graphical integration of Figure 8a,b and thereby estimate the total amount of each gaseous product: 0.94 mol of CH₄, 4.08 mol of CO, 8.54 mol of CO₂, 2.37 mol of H₂, 2.11 mol of O₂, and 37.17 mol of N₂. The amount of nitrogen was fixed by the measured amount of air delivered to the autoclave from the air accumulator. A total of 9.86 mol of oxygen was also delivered, of which 78.6% was consumed by combustion. Table 4 presents elemental analyses of the charcoal and carbonized charcoal products. The data

Table 4. Ultimate Analyses^a of the Charcoal and Carbonized Charcoal Products of Run LW-A2

	moisture ^b (%)	C (%)	H (%)	O (%)	N (%)	S (%)	ash (%)
charcoal	5.89	90.12	2.41	5.82	0.45	0.05	1.87
carbonized	5.77	92.14	1.55	3.91	0.44	0.07	1.92

^a All values in wt %. ^b Dry basis moisture content.

listed in Table 4 lead to the following material balance for Run LW-A2:



In this equation CH_{0.318}O_{0.048} represents the charcoal product (see Table 4) and its coefficient represents the experimental value of the charcoal yield (30%). This value differs slightly from the actual experimental value (29.5%) because we neglect ash, nitrogen, and sulfur in eq 4. Equation 4 accounts for 92.3% of the carbon in the feedstock. Some of the missing carbon is present in a liquid condensate (typically about 100 mL) composed primarily of water, but including some soluble organics, that collect in the cool lines leading to the exhaust port.

Closure of the oxygen and hydrogen balances is more difficult. The populations of hydrogen and oxygen atoms on the right side of eq 4 are 0.408 and 0.726 mol (respectively), while those on the left are 1.45 and 1.201 mol. The unaccounted differences are 1.042 and 0.475 mol, and the H/O ratio of the unaccounted difference is 2.19. This ratio is nearly identical to that of water. If we assume that water represents the missing hydrogen and oxygen, then the coefficient (α) of H₂O is between 0.475 and 0.521. This range of values is in good agreement with the coefficient of H₂O (0.475) on the left side of eq 2.

Compared to the values predicted to exist in thermochemical equilibrium (eq 2), higher yields of carbon monoxide and lower yields of methane and carbon dioxide were observed in this run (eq 4). The combustible gases contain 16.5% of the energy content of the Leucaena feed or 2981 kJ/kg of Leucaena. While this conversion of feed energy to gaseous product energy is about half that predicted for the carbonization of dry cellulose, the carbonization of *moist* Leucaena in this run created about 0.49 kg of steam/kg of Leucaena at 1 MPa total pressure. Shaft power can be recovered from this steam via a turbine.

We have seen that thermochemical equilibrium calculations can be used to predict the maximum value of the fixed-carbon yield from a biomass feedstock. But otherwise the predictions of these calculations have been misleading in the context of this work. For example, the thermochemical equilibrium calculations predict that elevated pressure should have no effect on the yields of carbon from biomass (see Figure 1a), yet the yields are significantly improved by carbonization at 1 MPa and above.⁴ Furthermore, air in the reactor during flash carbonization should preferentially attack the carbon (see Figure 5) and reduce its yield; but instead the yields are improved or remain the same. There are several explanations for these unexpected results. Biocarbons are composed of both a "primary" and a "secondary" carbon that is a coke derived from the decomposition of the tarry organic vapors onto the carbonaceous solid.^{19–21}

In the case of the primary carbon, water vapor or chemisorbed moisture may act as an autocatalytic agent for carbon formation from the biomass substrate at elevated pressures.^{12,14,22,23} Concerning the secondary carbon, under pressure the highly reactive, tarry vapors have a smaller specific volume; consequently, their intraparticle residence time is prolonged, increasing the extent of their decomposition as they escape the biomass particle. Also the concentration (partial pressure) of the tarry vapor is higher, increasing the rate of the decomposition reaction.¹² These effects are magnified when the flow of gas through the particle bed is small^{23,24}—as is the case at elevated pressure.^{25–27} Furthermore, the formation of secondary carbon from the tarry vapor is catalyzed by the charcoal;^{28–31} hence, the downward flow of the vapor through the hot, anaerobic carbon bed ensures a high conversion of these vapors to carbon. These kinetic phenomena underlie the unexpected improvement of fixed-carbon yields with increasing pressure. Similarly, mass-transfer limitations provide an explanation for the null effect of the presence of air on fixed-carbon yields. Although the thermochemical equilibrium calculations predict the preferential attack of oxygen on solid carbon, in reality the transport of oxygen to the carbon's surface is slow, whereas the mixing of oxygen with the pyrolysis gases is intimate and fast, and the gas-phase oxidation rates are enhanced by the elevated pressure. A more detailed inquiry into these findings is beyond the scope of the present paper, but will be a focus of future work.

Conclusion

1. Thermochemical equilibrium calculations predict the efficient conversion of biomass to carbon (charcoal). Using cellulose as a model compound, 62% of the carbon present in cellulose is transformed by pyrolysis into solid carbon when thermochemical equilibrium is established at 400 °C and 1 MPa. On an energy basis, 52% of the HHV of the cellulose is captured by the carbon product following the establishment of thermochemical equilibrium. Low temperatures and modest pressures favor the formation of carbon from cellulose.

2. When thermochemical equilibrium is attained at 400 °C and 1 MPa, the gaseous products of cellulose retain 7598 kJ/kg-cell of energy or 43.7% of the HHV of the cellulose feed, including 6313 kJ/kg-cell available as the HHV of the combustible product gas and 433 kJ/kg-cell available as work.

3. A packed bed of moist biomass contained in a pressure vessel can be ignited easily under an air pressure of 1 MPa. When the bottom of the bed is ignited, and air is delivered to the top of the bed, a flash fire quickly migrates up the bed—against the flow of air—triggering the transformation of the moist biomass to carbon (i.e., charcoal) and gas (i.e., steam, carbon dioxide, carbon monoxide, methane, and hydrogen). Under these circumstances, the fixed-carbon yield of charcoal throughout the bed can reach the thermochemical equilibrium “limit” in <30 min of reaction time. From the feedstocks studied in this work (Leucaena wood, oak wood, corncob, and macadamia nut shells) we realized charcoal yields ranging between 29.5 and 40.0%, fixed-carbon yields ranging from 27.7 to 30.9%, and energy conversion efficiencies of biomass to charcoal from 55.1 to 66.3%. Between 59 and 63% of the carbon in the feedstock was transformed to carbon in the charcoal. In all cases the charcoal product was uniform.

4. When moist (ca. 13%) Leucaena wood is carbonized, the product gas has a HHV of 3000 kJ/kg of dry Leucaena feed or 17% of the energy content of the Leucaena. Copious amounts of steam (e.g., 0.49 kg/kg of Leucaena) also are generated at elevated pressure (e.g., 1 MPa) during the flash carbonization of moist feedstocks that can be delivered to a turbine to generate shaft power.

5. Some of the findings reported herein were unexpected. For example, thermochemical equilibrium calculations predicted a negligible influence of pressure on charcoal yields, but we observed a significant improvement in yields under elevated pressure. Likewise, thermochemical equilibrium calculations predicted the preferential attack of oxygen in air at elevated pressure on the carbon product, but instead we observed the preferential attack of oxygen on the combustible gaseous products of pyrolysis. Common sense anticipates that moist biomass will offer lower yields of charcoal than dry biomass, but we observed little effect of the moisture content of the feedstock on the yield of charcoal (for the range of moisture contents studied). In a qualitative sense the high yields we observed resulted from improvements at elevated pressure in the rates of the pyrolytic carbonization reactions that consume the primary tars while producing carbon and light gases (secondary vapors) and from improvements at elevated pressure in the rates of combustion of the secondary vapors in the gas phase. Because of the high combustion rate of the secondary vapors in the presence of oxygen at elevated pressure, and mass-transfer limitations that prevent the oxygen from reaching the surface of the carbon, flash carbonization is a remarkably quick and efficient method for converting biomass into carbon.

6. We have assembled a demonstration reactor based upon a 0.9-m diameter × 2.7-m tall pressure vessel with a quick opening hinged closure that will be used to carbonize the University's green wastes while developing appropriate scaling laws for the flash-carbonization process. We hope to present results from this work soon.

Acknowledgment

We thank Prof. J. Brewbaker (University of Hawaii) for providing samples, Dr. G. Varhegyi (Hungarian Academy of Sciences), Dr. J. Benemann, D. Vahlsing (Kingsford/Clorox Corp.), and three anonymous reviewers for critical comments on the manuscript. This work was supported by the Coral Industries Endowment of the University of Hawaii.

Literature Cited

- (1) Antal, M. J.; Gronli, M. G. The Art, Science, and Technology of Charcoal Production. *Ind. Eng. Chem. Res.* **2003**, *42*, 1919.
- (2) Bard, E. Extending the Calibrated Radiocarbon Record. *Science* **2001**, *292*, 2443.
- (3) Antal, M. J.; Mok, W. S. L.; Varhegyi, G.; Szekely, T. Review of Methods for Improving the Yield of Charcoal from Biomass. *Energy Fuels* **1990**, *4*, 221.
- (4) Antal, M. J.; Allen, S. G.; Dai, X.; Shimizu, B.; Tam, M. S.; Gronli, M. G. Attainment of the Theoretical Yield of Carbon from Biomass. *Ind. Eng. Chem. Res.* **2000**, *39*, 4024.
- (5) Smith, K. R.; Pennise, D. M.; Khummongkol, P.; Chaiwong, V.; Ritgeen, K.; Zhang, J.; Panyathanya, W.; Rasmussen, R. A.; Khalil, M. A. K. Greenhouse Gases from Small-Scale Combustion Devices in Developing Countries: Charcoal-Making Kilns in Thailand. EPA-600/R-99-109; Office of Air and Radiation and Policy and Program Evaluation Div.: Washington, DC, 1999.

- (6) van der Plas, R. Burning Charcoal Issues. Energy Issues, FPD Energy Note No. 1; The World Bank Group: Washington, DC, 1995.
- (7) Bhattacharya, S. C.; Shrestha, R. M.; Sivasakthy, S. *State of the Art for Biocoal Technology*; Asian Institute of Technology: Bangkok, 1988.
- (8) Foley, G. *Charcoal Making in Developing Countries*; Earthscan: London, 1986.
- (9) Antal, M. J. Synthesis Gas Production from Organic Wastes by Pyrolysis/Steam Reforming. In *Energy from Biomass and Wastes*; D. L. Klass, Eds.; IGT: Chicago, 1978; p 495.
- (10) Desrosiers, R. Thermodynamics of Gas-Char Reactions. In *A Survey of Biomass Gasification*, SERI/TR-33-239; Reed, T. B., Eds.; NTIS: Springfield, VA, 1979; p II133.
- (11) Reynolds, W. C. *STANJAN Thermochemical Equilibrium Software*, 3.91.; Stanford University: Stanford, CA, 1987.
- (12) Mok, W. S. L.; Antal, M. J.; Szabo, P.; Varhegyi, G.; Zelei, B. Formation of Charcoal from Biomass in a Sealed Reactor. *Ind. Eng. Chem. Res.* **1992**, *31*, 1162.
- (13) Woolf, H. B., Ed., *Webster's New Collegiate Dictionary*, G.&C. Merriam Co.: Springfield, MA, 1975.
- (14) Antal, M. J.; Croiset, E.; Dai, X. F.; DeAlmeida, C.; Mok, W. S. L.; Norberg, N.; Richard, J. R.; Majthoub, M. A. High-Yield Biomass Charcoal. *Energy Fuels* **1996**, *10*, 652.
- (15) Antal, M. J., Jr. Process for Charcoal Production from Woody and Herbaceous Plant Material. U.S. Patent 5,435,983, 1995.
- (16) Cordero, T.; Marquez, F.; Rodriguez-Mirasol, J.; Rodriguez, J. J. Predicting heating values of lignocellulosics and carbonaceous materials from proximate analysis. *Fuel* **2001**, *80*, 1567.
- (17) Violette, M. Memoire sur les Charbons de Bois. *Ann. Chim. Phys.* **1853**, *32*, 304.
- (18) Violette, M. Memoire sur les Charbons de Bois. *Ann. Chim. Phys.* **1855**, *39*, 291.
- (19) Klason, P. Versuch einer Theorie der Trockendestillation von Holz. *J. Prakt. Chem.* **1914**, *90*, 413.
- (20) Hawley, L. F. *Wood Distillation*; Chemical Catalog Co.: New York, 1923.
- (21) Arseneau, D. F. Competitive Reactions in the Thermal Decomposition of Cellulose. *Can. J. Chem.* **1971**, *49*, 632.
- (22) Antal, M. J.; DeAlmeida, C.; Mok, W. S.-L. A New Technology for Manufacturing Charcoal from Biomass. In *Proceedings of the IGT Conference on Energy from Biomass & Wastes XV*; Klass, D. E., Ed.; Institute for Gas Technology: Chicago, 1991; p 521.
- (23) Varhegyi, G.; Szabo, P.; Mok, W. S.-L. Kinetics of the thermal decomposition of cellulose in sealed vessels at elevated pressures. Effects of the presence of water on the reaction mechanism. *J. Anal. Appl. Pyrol.* **1993**, *26*, 159.
- (24) Milosavljevic, I.; Oja, V.; Suuberg, E. M. Thermal Effects in Cellulose Pyrolysis: Relationship to Char Formation Processes. *Ind. Eng. Chem. Res.* **1996**, *35*, 653.
- (25) Mok, W. S. L.; Antal, M. J. Effects of Pressure on Biomass Pyrolysis. II. Heats of Reaction of Cellulose Pyrolysis. *Thermochim. Acta* **1983**, *68*, 165.
- (26) Blackadder, W.; Rensfelt, E. A Pressurized Thermo Balance for Pyrolysis and Gasification Studies of Biomass, Wood, and Peat. In *Fundamentals of Thermochemical Biomass Conversion*; Overend, R. P., Milne, T. A., Mudge, L. K., Eds.; Elsevier Applied Science: London, 1985; p 747.
- (27) Richard, J.-R.; Antal, M. J. Thermogravimetric Studies of Charcoal Formation from Cellulose at Elevated Pressures. In *Advances in Thermochemical Biomass Conversion*; Bridgwater, A. V., Eds.; Blackie Academic & Professional: London, 1994; p 784.
- (28) Xu, X.; Matsumura, Y.; Stenberg, J.; Antal, M. J. Carbon-Catalyzed Gasification of Organic Feedstocks in Supercritical Water. *Ind. Eng. Chem. Res.* **1996**, *35*, 2522.
- (29) Brandt, P.; Larsen, E.; Henriksen, U. High Tar Reduction in a Two-Stage Gasifier. *Energy Fuels* **2000**, *14*, 816.
- (30) Radovic, L. R.; Sudhakar, C. Carbon as a Catalyst Support: Production, properties, and applications. In *Introduction to Carbon Technologies*; Marsh, H., Heintz, E. A., Rodriguez-Reinoso, F., Eds.; Universidad de Alicante: Alicante, 1997; p 103.
- (31) Cookson, J. T. Physicochemical Changes of Substances By or Within Carbon Adsorption Beds. In *Activated Carbon Adsorption of Organics from the Aqueous Phase*; Suffet, I. H., McGuire, M. J., Eds.; Ann Arbor Science: Ann Arbor, 1980; p 379.

Received for review February 24, 2003

Revised manuscript received May 12, 2003

Accepted May 14, 2003

IE0301839